Research on lenses assemble precision in complicate laser amplification system

Tianzhuo Zhao (赵天卓)*, Ke Huang (黄 科), Zhijun Kang (康治军), Xue Zhang (张 雪), Yang Liu (刘 洋), Yunfeng Ma (麻云凤), Shuzhen Nie (聂树真), Jin Yu (余 锦), and Zhongwei Fan (樊仲维)**

Academy of Opto-electronics, Chinese Academy of Sciences, Beijing 100094, China

**Corresponding author: herachles@163.com; **corresponding author: fanzhongwei@aoe.ac.cn*

Received January 30, 2013; accepted March 10, 2013; posted online August 30, 2013

In a certain amplification system, signal laser can be amplified from 1 nJ to 5 J. To realize a high quality imaging transfer, meet beam diameter expansion requirement, and get good filtering effects, three spatial filters are designed and assembled. Lenses in these spatial filters can be assembled and adjusted by their reflection spots to meet wave-front requirements. In this letter, we analyze precision of the assembling, and make a ray-tracing simulation to discuss the relation between assembling precision and lenses parameters. On the optimized distance of 1000 mm, adjusting precision of lens tilt can reach 5 mrad.

OCIS codes: 120.0120, 120.1880, 140.0140, 140.3580, 140.3538.

doi: 10.3788/COL201311.S21203.

A laser beam with a flat-top intensity profile can be well amplified and is ideally suited for Ignition Confusion Facility (ICF). Generally speaking, in a long optical distance system where a uniform intensity distribution laser is required, gratings[1], distributive afocal lens[2] or other diffraction instruments[3] are primitive devices for beam shaping. Whereas these devices are passive and non-adjustable, cannot suit for thermal expansion caused by different pumping energy[4,5], which seriously limit their applications. Compared with said techniques, the beam shaping by use of liquid crystal spatial light modulators (LC-SLMs) has obvious advantages such as simplicity, suitable in realizing signal feedback and beam compensation through adjusting the electric parameters. However, although LC-SLMs technique has been widely addressed in recent years[6−9], LC-SLMs device for beam shaping and compensation is few reported. In our previous work, we reported the theoretical simulation and experiment of beam shaping by a LC-SLM device, and a Gaussian distributed laser beam with single pulse energy of 1 nJ was successfully amplified to 5 J with a flat top beam profile of 50×50 (mm) in dimension[10,11]. In this work, we make a further report on the assembling of the image transfer system.

Four levels of amplifiers constitute the amplification system. Firstly, a 1-nJ, 3-ns, 1-Hz, 1 053-nm seed fiber laser train was injected into the initial amplifier and was amplified to 30 mJ by the first and the second amplifiers. After suitable beam expanding it was projected onto a LC-SLM (LC2002, Holoeye Co. Ltd., Germany). The LC-SLM is composed of 832×624 (pixel) with the pixel pitch of 32 μm. The available area of the LC valve is 26.6×20.0 (mm). Damage threshold of the LC valve is about 2 W/cm^2. Secondly, the shaped laser beam was re-amplified to about 700 mJ by a dual-pass traveling-wave amplification module (the 3rd amplifier). The 3rd amplifier modules used Nd:glass slice as working material, and it was end-pumped by a laser diode stack with a duct for coupling. Finally, the laser was ultimately amplified to >5 J after another dual-pass amplification module (the 4th amplifier). The 4th amplifier modules use Nd:glass as working materials and use arc-lamp for side-pumping. During the beam propaganda, the laser was modulated and expanded by three spatial filters (PSF1, PSF2, and PSF3), sequentially. Optical theory structure with four amplifier levels and three PSFs was shown in Fig. 1. Coupling lens was used between signal laser input fiber and the first amplifier to adjust the input signal. Beam expender was used in front of LC-LSM to meet low energy damage requirements of it. PSF1, PSF2, and PSF3 were used among the third amplifier, the forth amplifier, and main amplifier to change beam size and realize the function of special filter. Transmission efficiency of every point on LC-LSM can be controlled, and this was used to revise finally output of the main amplifier. Therefore the special filter using in the per-amplifier need transmit the image of LC-LSM well to main amplifier to realize a precisely optimization of the finally energy output distribution.

Based on design requirements, PSF1 would make an image of LC-LSM on high reflection mirror HR2, and this image would be delivered to HR3 by PSF1 and PSF2. PSF3 will continuous transmit the image of LC-LSM from HR3 to main amplifier. To meet the requirements of root mean square (RMS) wavefront aberration lower than $\lambda/6$, lenses parameters are calculated, and tolerance requirements are distributed.

During the course of assembling, when a lens is tilted or off axis, reflection spots of two surfaces cannot hold on the optical axis at the same time. If the lens is tilted or off-axis seriously, reflection spot center position can be used to judge lens position. When the lens is tilted or off-axis not so seriously, interference will be obvious between reflection spot of two sides of the lens. Judging by the center of interference fringes, position of the reflection focusing spot can be adjusted more easily and precisely. If θ denotes the divergence of the assembling laser, and D_0 is the initial spot size (Fig. 2), after a distance of l, spot size on the lens can be

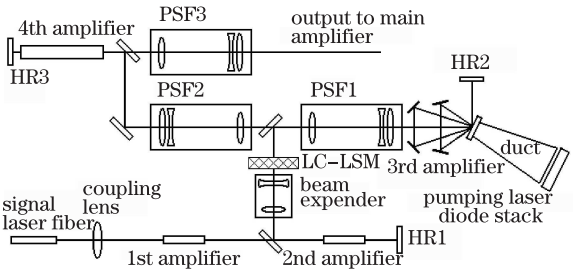

Fig. 1. Structure scheme of amplifier and special filter in the amplification system

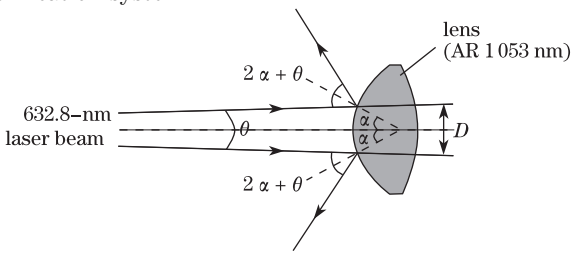

Fig. 2. Reflection spot characters on the first surface of alignment lens.

$$D = l \cdot \theta + D_0. \tag{1}$$

In this case, incidence of marginal rays is

$$\alpha = \arcsin \frac{D}{2R_1}, \tag{2}$$

where R_1 represents curvature radius of the first surface. After reflection, beam divergence of assembling laser enlarge to $2\theta + 4\alpha$. To a convex surface, after a collimator distance of L, spot radius is

$$r = L\left(\theta + 2\arcsin\frac{D}{2R}\right). \tag{3}$$

For example, to a convex lens with a front radius of R=50 mm, assembling laser half divergence is 1.5 mrad, and diameter of the spot size on the lens is 2.3 mm, spot sizes on the distance of 1 000, 500, and 200 mm are 97.3, 49.8, and 21.3 mm, respectively. If similarly considered that spot overlapping precision is 10% of the spot size without influence by distance, assembling error can be 9.73, 9.96, and 10.7 mrad. Relations between alignment angle, different collimator distance and curvature radius are shown in Fig. 3. Overall, alignment angle is mainly determined by curvature radius of the lens. If curvature radius is too small, reflection spot is too big, and this causes reflection spot center is hard to be overlapped with optical axis, this will dramatically decrease alignment precision. To a certain lens, if collimator distance is prolonged, alignment precision can be slightly improved, and we regard 1 000 mm as an optimized collimator distance. Furthermore, if a narrower beam be used to alignment, precision could be higher. On the other hand, if the front surface of the lens is a concave surface, a negative R value should be used. In the certain case, relation between assembling beam divergence and enlargement caused by creature reflection is subtraction, therefore, alignment precision will be higher. No matter concave or convex, curvature radius is the most important factor which influenced alignment precision.

In course of alignment, the second surface of the lens will also reflect a part of energy back. After going through the lens, the spot can be observed by putting a screen between alignment laser source and the lens in most cases. Also consider θ as the divergence of the assembling laser, and D as the spot size on the lens, R_1 represents curvature radius of the first surface, R_2 represents curvature radius of the second surface, distance from screen to the lens is l, thickness of the lens is d, incident angle on the first surface is the same as Eq. (2):

$$\alpha_1 = \theta + \arcsin\frac{D}{2R_1}. \tag{4}$$

Emergence angle is

$$\alpha_1' = \arcsin\left[\frac{n_1}{n_2}\sin\left(\theta + \arcsin\frac{D}{2R_1}\right)\right]. \tag{5}$$

If regards

$$\beta_1 = \arcsin\frac{D}{2R_1}, \tag{6}$$

then the divergence of marginal ray in the lens is

$$\beta_1 - \alpha_1' = \arcsin\frac{D}{2R_1} - \arcsin\left[\frac{n_1}{n_2}\sin\left(\theta + \arcsin\frac{D}{2R_1}\right)\right], \tag{7}$$

and marginal ray height is

$$\frac{D_1}{2} = \frac{D}{2} - d_1\mathrm{tg}(\beta_1 - \alpha_1'), \tag{8}$$

where d_1 is the thickness of the marginal ray light in the lens, as shown in Fig. 3. It can be gotten through the equation set:

$$\begin{cases} \dfrac{\frac{D}{2} - \frac{D_1}{2}}{d_1} = \mathrm{tg}(\beta_1 - \alpha_1') \\ d_1 = d - \dfrac{D}{2}\mathrm{ctg}\beta_1 - \dfrac{D_1}{2}\mathrm{ctg}\beta_2 \\ \beta_2 = \arcsin\dfrac{D_1}{2R_2} \end{cases}.$$

Incident angle and reflection angle on the second surface is

$$\alpha_2 = \alpha_2' = \beta_1 - \alpha_1' + \beta_2, \tag{9}$$

and the divergence between reflected light and optics axis is

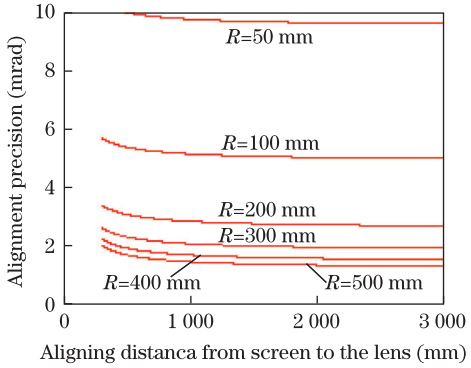

Fig. 3. Collimator distance and curvature radius as the function of alignment angle.

$$\alpha_2' + \beta_2. \tag{10}$$

After going through the first surface, the incident angle is

$$\alpha_3 = \alpha_2' + \beta_2 + \beta_3, \tag{11}$$

and the marginal ray height is

$$\frac{D_2}{2} = \frac{D_1}{2} - d_2 \mathrm{tg}(\alpha_2' + \beta_2), \tag{12}$$

where d_2 is the thickness of the marginal ray light in the lens, when it reflects back, as shown in Fig. 3. It can be gotten through the equation set:

$$\begin{cases} \dfrac{\frac{D_1}{2} - \frac{D_2}{2}}{d_2} = \mathrm{tg}(\alpha_2' + \beta_2) \\ d_2 = d - \dfrac{D_1}{2}\mathrm{ctg}\beta_2 - \dfrac{D_2}{2}\mathrm{ctg}\beta_3 \\ \beta_3 = \arcsin\dfrac{D_2}{2R_1} \end{cases}$$

Finally, emergence angle on the first surface is

$$\gamma = \alpha_3' - \beta_3 = \arcsin\left(\frac{n_2}{n_1}\sin\alpha_3\right) - \arcsin\frac{D_2}{2R_1}. \tag{13}$$

Figure 4 is gotten from the calculation of ZEMAX. The beam divergence is 1.5 mrad, spot diameter is 2.3 mm, and choosing radius of the second surface as horizontal ordinate, with a range from 50 to 1 000 mm, longitudinal ordinate is the spot radius. With the increasing of curvature radius, the size of the spot reflected by the second surface is decreased, from 50 to 4.7 mm.

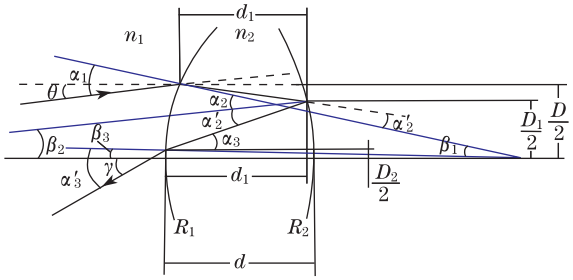

Fig. 4. Reflection spot characters on the second surface of alignment lens.

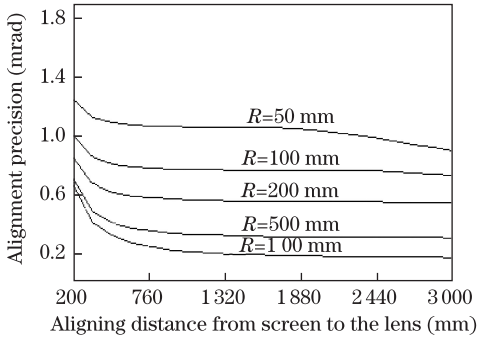

Fig. 5. Relation between spot radius and different curvature radius of the second surface.

After calculating with different curvature radii of the second surface and different alignment distance, Fig. 5 can be gotten. In Fig. 5, horizontal ordinate presents alignment precision of lens tilt, and the unit is mrad. From the curve we can know that alignment precision of a R_2=1 000 m lens can reach 0.3 mrad, and to a lens with R_2=100 mm, alignment precision is about 0.9 mrad. To a certain lens, if collimator distance is prolonged, alignment precision can be slightly improved, and we regard 2 000 mm as an optimized collimator distance. If curvature radius of the second surface is bigger, alignment precision changes faster. Distance is not the most important factor, but precision is mainly determined by curvature radius of the second surface. Furthermore, contrasting with Fig. 3, Fig. 5 also shows that using the focusing point of the second surface of the lens for alignment can get a higher precision.

In conclusion, during the course of alignment, tilt and off-axis problems exist in the same time. Lose sight of deviations induced by manufacturing, tilt and off-axis can induce one reflective spot on the optical axis. It means that if one reflective spot is adjusted on the optical axis, perhaps tilt and off-axis still exist at the same time. If two reflective spots hold on the optical axis in the same time, tilt and off-axis errors will be solved. When off-axis are considered, further calculations should be made.

This work was supported by Scientific Equipment Development Project of Chinese Academy of Sciences (No. YZ201216), and Science and Technology Project of Haidian Distinct, Beijing (No. K20110037)

References

1. Y. Park, M. Kulishov, R. Slavík, and J. Azañ, Opt. Express **14,** 12670 (2006).
2. D. Shafer, Opt. Laser Tech. **14,** 159 (1982).
3. S. W. Bahk, E. Fess, B. E. Kruschwitz, and J. D. Zuegel, Opt. Express **18,** 9151 (2010).
4. M. R. Taghizadeh, P. Blair, K. Balluder, A. J. Waddie, P. Rudman, and N. Ross, Opt. Laser. Eng. **34,** 289 (2000).
5. P. Villoresi, S. Bonora, M. Pascolini, L. Poletto, G. Tondello, C. Vozzi, M. Nisoli, G. Sansone, S. Stagira, and S. De Silvestri, Opt. Lett. **29,** 207 (2004).
6. S. Bonora, D. Coburn, U. Bortolozzo, C. Dainty, and S. Residori, Opt. Express **20,** 5178 (2012).
7. J. Bourderionnet, A. Brignon, J. P. Huignard, A. Delboulbé and B. Loiseaux, Opt. Lett. **26,** 1958 (2001).
8. N. Sanner, N. Huot, E. Audouard, C. Larat, J.-P. Huignard, and B. Loiseaux, Opt. Lett. **30,** 1479 (2005).
9. S. Residori, A. Petrossian, T. Nagaya, and M. Clerc, J. Opt. B: Quantum Semiclass. Opt. **6,** S169 (2004).
10. Y. Ma, Z. Fan, J. Qiu, C. Feng, T. Zhao, and W. Lin, Chin. Opt. Lett. **8,** 134 (2010).
11. T. Z. Zhao, J. Yu, C. Y. Li, K. Huang, Y. F. Ma, X. X. Tang, and Z. W. Fan, J. Modern Opt. **60,** 109 (2013).